

Incorporation of Material Model into LS-DYNA Implicit to Model the Shear Behavior of Uncured Woven-Fabric Composite Materials

Jennifer L. Gorczyca, James A. Sherwood, Darin S. Lussier, Julie Chen

Advanced Composite Materials and Textile Research Laboratory
Department of Mechanical Engineering
University of Massachusetts Lowell

Corresponding Author:

James A. Sherwood

Mailing address:

Department of Mechanical Engineering

University of Massachusetts-Lowell

One University Ave.

Lowell, MA 01854

Telephone: 978-934-2584

Email: James_Sherwood@uml.edu

Keywords: composite material, finite elements, user material model, woven fabric

ABSTRACT

A shear-frame FE model for use in the LS-DYNA implicit code was created to predict the forming behavior of an uncured woven-fabric composite material. This FE model contains fully integrated shell elements and beam elements. A material model developed by McBride and Chen for plain-weave woven composite materials and later refined by Bulusu and Chen to account for different fabric weaves was incorporated into LS-DYNA implicit to model the behavior of a 40-60 glass-polypropylene satin-weave fabric as the fabric deformed in a shear-frame experiment. The normalized force-displacement results from the FE model were compared to the experimental results.

INTRODUCTION

Credible material models are readily available in commercial FEA packages for cured woven-fabric reinforced composites. However, these same material models are not applicable for the uncured state of such composites because they cannot capture orders of magnitude changes in material properties as the uncured composite is formed through processes such as stamping.

Many woven-fabric material models exist in open literature, but most are limited to specific geometrical shapes, loading conditions and/or fabric geometries. Thereby, limiting their value for general FE analyses. A few citations exist for robust woven-fabric material models having the potential for incorporation into FEA packages for general analyses, but such incorporation has yet to be realized.

The motivation for incorporating this type of material model for use in a commercial FEA code is to create a design tool widely available to industry and researchers. Woven-fabric reinforced composite materials are of interest because they can be used to mass produce strong lightweight low-cost components using forming methods such as stamping. When woven fabrics are stamped, the main mode of deformation is shear (Figure 1). For this reason, the shear properties of the fabric and the ability to predict these properties are of great importance.



Figure 1. The main mode of deformation when a woven fabric is stamped is shear

EXPERIMENT

The following subsections describe the development of the material model that was incorporated into LS-DYNA for the shear frame FE model, the creation of the shear frame FE model and the comparison of the numerical results to the experimental results, respectively.

Material Model

A material model developed by McBride and Chen (1997) for plain-weave woven composite materials and later refined by Bulusu and Chen (2000) to account for different fabric weaves was incorporated into LS-DYNA implicit. This customized program was subsequently used to model the mechanical behavior of a satin-weave fabric.

Using the McBride-Chen (1997) material model, the effective constitutive matrix of a plain-weave fabric reinforced composite during the forming process can be determined starting with the properties of a single yarn. The model assumes that each yarn follows a sinusoidal path with no gaps or spacings between the yarns (Figure 2). In addition, the cross-section of a unit cell shows that the yarns are lenticular in shape.

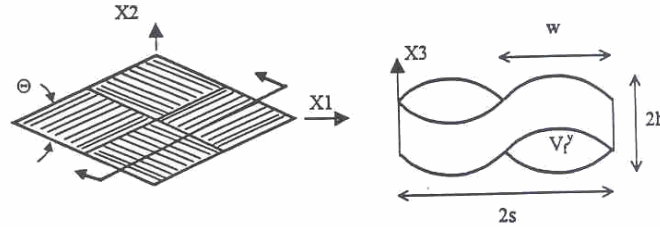


Figure 2. Top view and side view of unit cell of plain-weave fabric

To determine the deformation behavior of a fiber bundle or a yarn from the fibers within a yarn, McBride and Chen incorporated Cai and Gutowski's (1992) model, based on beam theory. With this model, the original, current, and final fiber volume fractions within the yarn are calculated. These values are then used to determine the transverse, axial, and Poisson effect compliance terms for a transversely isotropic aligned yarn. To account for varying amounts of waviness in the fibers that compose a yarn, a fiber waviness coefficient, β , must be determined. The material parameter β , represents the ratio of the length of the fiber unit cell to the height of the unit cell minus the diameter of the fiber in the unit cell (Eq. 1). Figure 3 shows a representative fiber cell.

$$\beta = \frac{L}{h - d} \quad \text{Eq. 1}$$

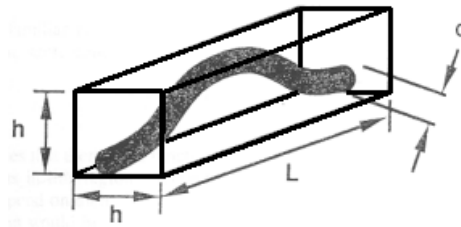


Figure 3. Representative fiber unit cell as shown by Cai and Gutowski

Cai and Gutowski's model was then extended to account for all the fibers that exist in a unit cell. Applying strains and stresses, the compliance matrix C_{ij} was determined to satisfy Eq. 2.

$$d\sigma_{ij} = C_{ij} d\varepsilon_{ij} \quad \text{Eq. 2}$$

The compliance matrix was then extended to the whole fabric by McBride and Chen using the Orientation Averaging Technique, which is based upon the theory that the fabric is a homogeneous material undergoing 'iso-strain'. At this stage, the average constitutive tensor for a unit cell of plain-weave fabric is determined by discretizing each yarn into a minimum of 20 slices (Figure 4). The resulting effective constitutive tensor for a unit cell of fabric is multiplied by the average strain increment (an input) and used to calculate the average stress increment (Eq. 3).

$$(\Delta\sigma_{ij})_{\text{avg}} = C_{ij} (\Delta\varepsilon_{ij})_{\text{avg}} \quad \text{Eq. 3}$$

Thus, as the deformation occurs at the microscopic level through the changing angles between the tows, the macroscopic properties of the entire fabric evolve.

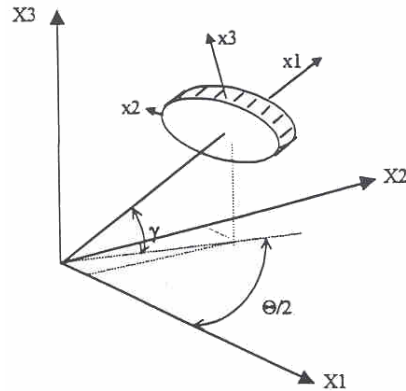


Figure 4. Representative slice of a yarn used for Orientation Averaging Technique

The Bulusu-Chen material model expands upon the McBride-Chen material model to account for different fabric architectures. Bulusu and Chen used cubic-spline interpolation to calculate the yarn path in a unit cell for a specific fabric weave. This model also accounts for gaps between warp and weft tows. **Error! Reference source not found.** shows a calculated yarn path applying this model to a satin-weave fabric.

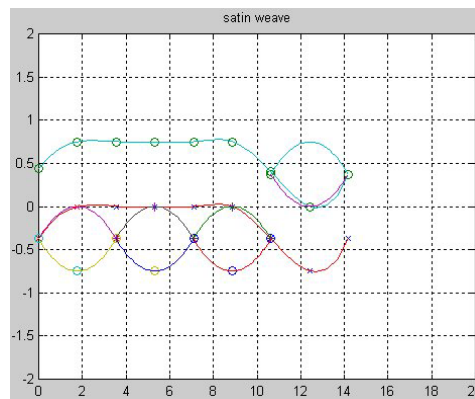


Figure 5. Cross-section of unit cell in a satin-weave fabric as represented by Bulusu-Chen material model.

Finite Element Model

Before a process as complex as stamping of a woven-fabric composite can be modeled, it is necessary to validate the material model for a simpler situation. Because the main mode of deformation of a woven fabric is shear, it was decided that the material model should be first validated for a fabric in shear.

A shear-frame FE model for use in the LS-DYNA implicit code was created to predict the forming behavior of an uncured woven-fabric composite material. This FE model contains 96 shell elements and 40 beam elements. Displacements are prescribed on the left and right corner nodes. Thus, kinematics dictate the motion of the top and the bottom corner nodes (Figure 5). Currently, the fabric is modeled using fully integrated shell elements. At this point, it is important to note that the fabric deformation is a plane-stress problem. Thus, membrane elements are traditionally used in the formulation. However, at the writing of this paper, LS-DYNA Implicit did not support membrane elements.

Finally, the displacement of the fabric is constrained to the x-y plane, as the model did not converge prior to placing this constraint on the associated elements. Hence, this FE model is currently limited to analyses for which fabric wrinkling does not occur (i.e. the range of fabric deformation prior to the locking of the yarns).

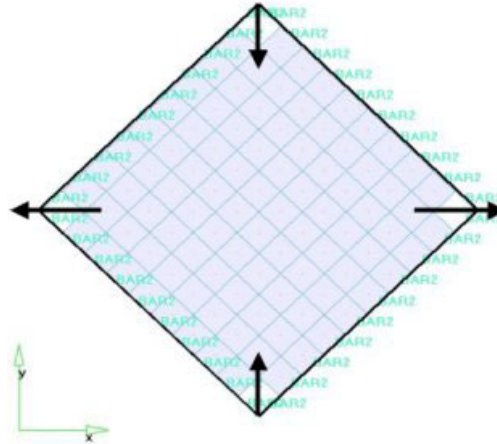


Figure 5. Shear Frame FE Model

Numerical experiments were also run on a simplified version of this shear frame model. The simplified model contained one element placed under displacement boundary conditions at each of the four corners. The displacements of the corners of the simplified one-element model were chosen to match the displacement of the 96-element finite element model.

Shear Frame Experiment

Shear-frame experiments were conducted at room temperature on plain- and satin-weave fabrics consisting of commingled polypropylene-glass fibers (Figure 6). The results are expressed in terms of force-displacement curves normalized by the area of the fabric in the unnotched portion of the fabric (Chow, Lussier and Chen, 2001).

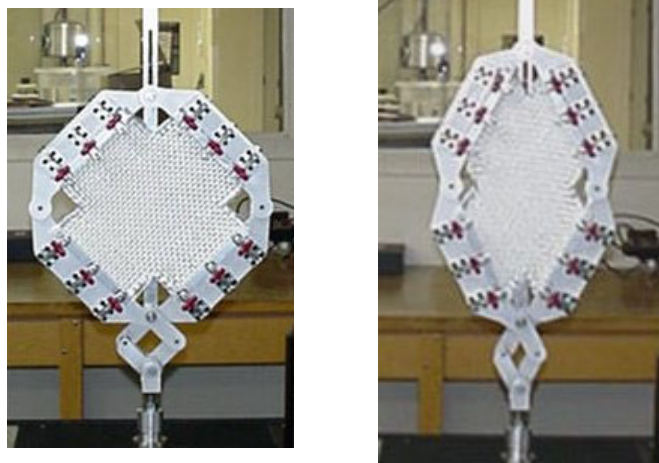


Figure 6. Shear Frame

RESULTS

The initial force-displacement results from the finite element model of the shear frame are compared to the experimental force-displacement results in Figure 7. Note the similarity between the shapes of the curves resulting from the experimental data and the data obtained from the finite element model. To show this comparison, however, it is important to note that the finite element results are overpredicting the experimental fabric stiffness by seven orders of magnitude.

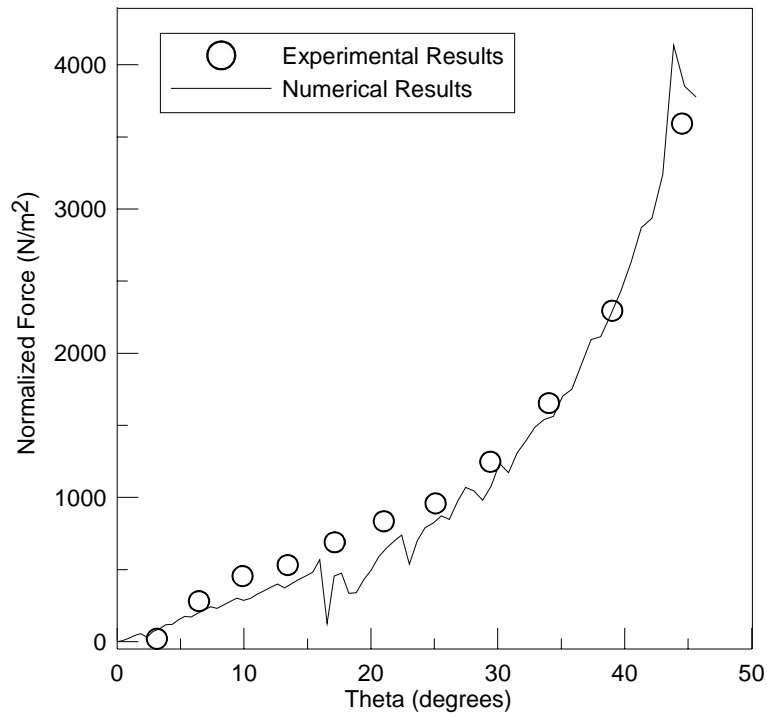


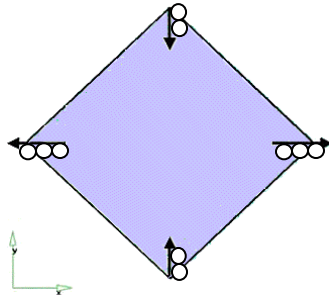
Figure 7. Comparison between numerical and experimental results

It was also noted that large forces were deforming the beam elements used to model the shear frame. These elements were elongating. Thus, the authors first attempted to strengthen the frame by increasing the thickness of the beams. However, increasing the thickness of the frame to a point such that it would not deform resulted in nonconvergence problems. The authors believe that this nonconvergence situation was due to a numerical instability resulting from relatively large values on the main diagonal of the stiffness matrix associated with the beam elements in comparison to the stiffness values associated with the fabric elements.

The authors next investigated the potential reasons for this overprediction of the force required to deform the fabric in shear. The first part of the investigation involved simplifying the finite element model. In the second part of the investigation, models were generated to investigate the material parameter β because it was known from previous numerical studies that as β increased the calculated force required to deform the fabric decreased.

Altering the Finite Element Model

In an attempt to simplify the finite element model for investigating the reasons for the large discrepancy between the finite element model results and the experimental results, a finite element model consisting of one element placed in shear was generated. So that the single element would shear without stretching, an additional set of displacement boundary conditions was added on the top and bottom nodes. It was desired to replace the beam elements used for the frame for two reasons. The authors wanted to avoid the issues associated with nonconvergence that resulted when the stiffness of the fabric and the stiffness of the shear frame were significantly different from each other, and they wanted to avoid effects on the results due to the stretching of the beams, which resulted when the beams were essentially rigid in comparison to the fabric. The size of this one-element model was chosen to be equal to the size of the un-notched specimen in order to obtain results applicable for comparison, as the un-notched portion of the specimen is responsible for the resistance to deformation when placed in the shear frame (Figure 8). It was acceptable to generate and run a one-element finite element model such as this because the behavior of the fabric when placed in a shear frame is commonly assumed uniform across the fabric for any displacement.



Single-element FE model for shear response of fabric. Displacements are prescribed on all four corner nodes as shown such that the length of each side remains constant throughout the deformation.

Figure 8. Single-element FE model.

β Investigation

Recall as previously discussed, β is the fiber-waviness material parameter. Thus, the value of β has a physical significance. It is determined empirically so as to obtain a value for S22 from an experiment that matches the theoretical S22 value. Applying the conditions of constrained compression, the value of the transverse stiffness of the yarn is calculated from the experimental data using Eq. 4.

$$S22 = \frac{\epsilon_z}{(1 - \nu_{TT}^2) \sigma_z} \quad \text{Eq. 4}$$

where ν_{TT} is the transverse Poisson's ratio and is equal to 0.8. The experiment generates the values of ϵ_z and σ_z , which are used to compute the experimental value of S22. Eq. 5 is the theoretical equation for S22 developed by Bulusu and Chen.

$$S22 = \frac{\frac{\beta^4}{3\pi E} \left(\sqrt{\frac{V_a}{V_f}} - 1 \right)^5}{\sqrt{\frac{V_a}{V_f}} \left(5 - \sqrt{\frac{V_f}{V_a}} - 4 \sqrt{\frac{V_o}{V_f}} \right)} \quad \text{Eq. 5}$$

where V_o , V_f and V_a are the minimum, current and maximum fiber-volume fractions, respectively, for square packing, and E is the elastic modulus for the fibers. The predicted and experimental values of S22 are compared for various values of β . The value of β for which the best correlation is obtained between the theoretical and experimental values of S22 is taken to be the optimum value for glass yarns.

Because β was determined through an empirical procedure to match theoretical values with experimental data, it was decided to investigate the effect of varying β in the FE model on the force-displacement results. Perhaps a different value for β could lead to a better correlation between the experimental results and the FE model results.

It was noted that increasing the value of β , decreased the stiffness of the fabric. Thus, the force required to deform the fabric in the shear frame would be reduced. Cai and Gutowski reported that β ranged from approximately 100 to 300 for graphite fibers. Hence, models were run with various values of β starting within that range and extending above it. It was noted that the effect of increasing β to reduce the forces in the force-displacement curve was essentially insignificant for values of β over 500. The curvature in the force-displacement relation diminishes as β increases (Figure 9). The resulting force-displacement curve for β equal to 500 was still six orders of magnitude larger than the experimental force-displacement curve. Thus, the authors are investigating other ways to resolve the discrepancy between the FE and experimental force-displacement curves.

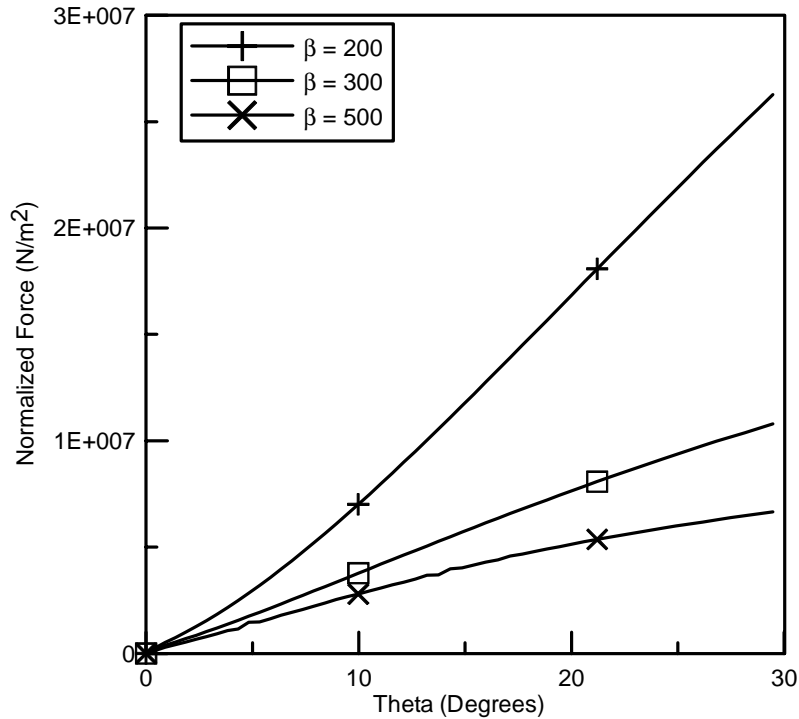


Figure 9. Effect of varying β on force-displacement curve for single element FE model

CONCLUSIONS

In conclusion, a fabric material model exists which can be used as a user-defined material model in LS-DYNA. However, when combined with the FE method in the material models present formulation, it overpredicts the effective fabric stiffness. Investigations were conducted into altering the material parameter β to explore its potential for improving the correlation between experimental and FE results. The influence of β became insignificant before correlation could be achieved.

ACKNOWLEDGEMENTS

Funding for this work was obtained from the NSF GOALI program in cooperation with Ford Motor Company. The help from Brad Maker and Pat Kulzer of LSTC is appreciated.

REFERENCES

- Bulusu, A. and Chen, J. (2000). "Fabric Architecture and Shear Deformation Analysis of Woven-Fabric Composites During Forming." ASC 15th Technical Conference Proceedings.
- Cai, Z. and Gutowski, T. (1992). "The 3-D Deformation Behavior of a Lubricated Fiber Bundle." Journal of Composite Materials, Vol. 26, pp. 1207-1237.
- Chow, S., Lussier, D. and Chen, J. (2001). "Shear and Friction Response of Co-Mingled Glass/Polypropylene Fabrics During Stamping." ASC 16th Technical Conference Proceedings. pp. 169-171.
- McBride, T. and Chen, J. (1996). "Yarn geometry and volume fraction evolution during composites forming." Proceedings of the 1996 ASME International Mechanical Engineering Congress and Exposition, pp. 43-44.
- McBride, T. and Chen, J. (1997). "Unit-cell geometry in plain-weave fabrics during shear deformations." Composites Science and Technology, Vol. 57, pp. 345-351.